Doping dependence of the chemical potential in cuprate high-T_c superconductors
II. $(Bi, Pb)_2Sr_2Ca_2Cu_3O_{10+\delta}$

G. Rietveld [a,b,*], S.J. Collocott [c], R. Driver [c], D. van der Marel [a,d]

[a] Delft University of Technology, Department of Applied Physics, Lorentzweg 1, 2628 CJ Delft, The Netherlands
[b] NMi-Van Swinden Laboratorium, Department of Electrical Standards, PO Box 654, 2600 AR Delft, The Netherlands
[c] CSIRO, Division of Applied Physics, Lindfield, 2070 Australia
[d] Materials Science Centre, Solid State Physics Laboratory, University of Groningen, Nijenborgh 4, 9747 AG Groningen, The Netherlands

Abstract

Using X-ray photoelectron spectroscopy, a systematic study is performed of the doping dependence of the chemical potential μ in $(Bi, Pb)_2Sr_2Ca_2Cu_3O_{10+\delta}$. The doping is varied by changing the oxygen content of the sample. The measured shift of the chemical potential is compared with present models for the doping behavior of μ in high-T_c materials. Our results show best agreement with the model in which the chemical potential is assumed to shift upon doping the parent insulating material.

1. Introduction

This paper is a sequel to Ref. [1], where we studied the doping dependence of the chemical potential in $La_{2-x}Sr_xCuO_4$ as a function of Sr content. The aim of such studies is to shed light on the character of the states that are created near the Fermi level upon doping in the high-T_c superconductors. Up to now, two models have been proposed for describing the doping behavior of the chemical potential in these materials. The "impurity model" assumes that impurity-induced states are created near the Fermi level upon doping, filling the originally empty charge-transfer gap. Hence, the chemical potential will be more or less constant, near the middle of the gap. In the "semiconductor model" it is assumed that the increase in the density of states near the Fermi level upon (hole) doping is mainly caused by a shift of the chemical potential into the valence band. Here, the character of the states near the Fermi level thus is determined by the states in the top of the valence band. Both the "impurity model" and the "semiconductor model" are supported by experiments, namely by measurements on $Nd_{2-x}Ce_xCuO_4$ [2,3] and $Bi_2Sr_2Ca_{1-x}Y_xCu_2O_{8+\delta}$ [4], respectively.

In the present paper we present measurements of the behavior of the chemical potential as a function of doping in $(Bi, Pb)_2Sr_2Ca_2Cu_3O_{10+\delta}$. Here, the doping is varied by annealing a sample in different oxygen atmospheres. As in the previous article, we will first discuss preparation and characterization of the sample, and subsequently the X-ray photoelectron spectroscopy (XPS) measurements and the behavior of the chemical potential in this material.

* Corresponding author.

2. Preparation and characterization

The family of $Bi_2Sr_2Ca_nCu_{n+1}O_{2n+6+\delta}$ materials is particularly suited for XPS studies because they are relatively inert and not sensitive to moisture and other contaminants in the environment. On the other hand it is difficult to prepare single-phase material. The early Bi–Sr–Ca–Cu–O samples predominantly contained the $n=1$ material, with certain fractions of the $n=0$ and $n=2$ phases, depending on the preparation. Later it was found that the addition of Pb stabilizes the structure. Especially the $n=2$ material, used in this study, cannot be made single phase without this addition.

Our $(Bi, Pb)_2Sr_2Ca_2Cu_3O_{10+\delta}$ sample is prepared by a two-step ceramic route starting from Bi_2O_3, PbO, $SrCO_3$, $CaCO_3$ and CuO powders of approximately 99% purity. A Pb free Bi–Sr–Ca–Cu–O precursor was first prepared by calcination at 800 and 840°C. The required amount of PbO was then added, and a final sintering was performed in air at 860°C, and then 850°C for a total of 80 h [5]. The nominal composition of the sample, as determined from the starting composition of the oxides in the preparation, is $Bi_{1.84}Pb_{0.34}Sr_{1.91}Ca_{2.03}Cu_{3.06}O_{10+\delta}$.

The sample was given four different surface preparation treatments in our ultra-high vacuum (UHV) system, resulting in four different values of the oxygen content as determined from the relative intensities of the XPS lines. The sample surface was freshly scraped in situ with a sapphire plate, each time before it was heated and/or exposed to ozone. The pressures and temperatures used in the ozone anneals are typical for in-situ growth of high-quality $YBa_2Cu_3O_{7-\delta}$ thin films in our system [6]. The freshly scraped surface always exhibited almost the same set of XPS spectra, from which we conclude that the changes in oxygen content due to heat/ozone treatment are the strongest in a top layer thinner than the "scraping" depth (about 0.1 mm).

Treatment A consisted of scraping of the as-prepared sample in UHV, without any extra heat or ozone treatment. In treatment B the sample was heated to 330°C in 3×10^{-4} mbar ozone for 15 min, and the ozone delivery was stopped during cool-down. Treatment C was to anneal the sample at 450°C in 6×10^{-4} mbar ozone for 20 min, and cool down to room temperature in the same ozone atmosphere.

Treatment D consisted of heating to 100°C in UHV for 15 min. The lower temperature for this vacuum anneal was chosen as the $(Bi, Pb)_2Sr_2Ca_2Cu_3O_{10+\delta}$ material is known to decompose when heated to high temperatures at low oxygen pressures.

We have characterized the sample with X-ray diffraction and resistance measurements before it was introduced in the UHV system, and after the total series of surface treatments and XPS measurements was completed.

The X-ray powder diffraction pattern of the as-prepared sample is displayed in Fig. 1. All peaks can be assigned to the $n=2$ material. There is no indication of the presence of an $n=1$ phase, which is the most frequently found impurity in $Bi_2Sr_2Ca_3Cu_3O_{10+\delta}$ samples. This is best visible from the narrow $(00\underline{14})$ peak, which is considerably broadened by the $(00\underline{12})$ peak of $Bi_2Sr_2CaCu_2O_{8+\delta}$ if this material is present. A least-squares fit to the peak positions using a tetragonal unit cell, gives for the lattice parameters $a = 5.403 \pm 0.002$ Å and $c = 37.02 \pm 0.02$ Å, which are typical values found for this material.

The resistance was measured with a standard four-terminal technique. The data shown in Fig. 2 are plotted relative to the resistance at 300 K. For the as-prepared sample the resistance curve is almost linear above T_c. The onset critical temperature is 110 K. Zero resistivity is obtained at 99–103 K, slightly depending on the magnitude of the measuring current
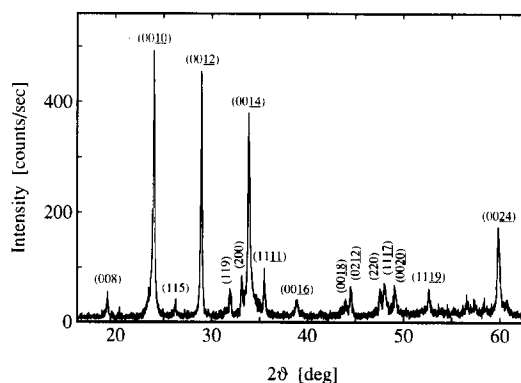

Fig. 1. X-ray powder diffraction pattern of the $(Bi, Pb)_2Sr_2Ca_2Cu_3O_{10+\delta}$ sample directly after preparation. All peaks can be ascribed to the $n=2$ material; impurity phases, such as the frequently found $n=1$ phase, are absent. The majority of the peaks is labeled with their Miller indices. Cu Kα radiation with a Ni filter was used in the measurement.
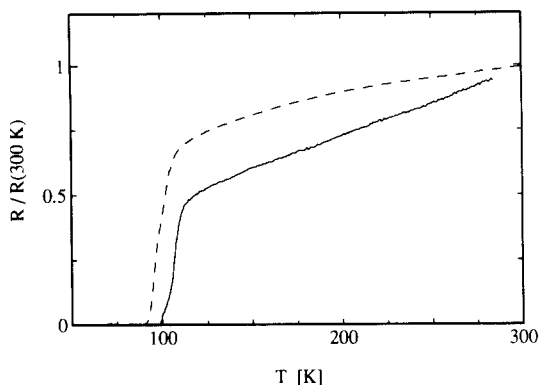
Fig. 2. Temperature-dependent resistance measurements of (Bi, Pb)$_2$Sr$_2$Ca$_2$Cu$_3$O$_{10+\delta}$ relative to the resistance at room temperature for the as-prepared and the vacuum-annealed sample (solid and dashed line, respectively). After vacuum anneal, both the lower T_c and the non-linear behavior of the resistance above T_c indicate a lower quality of the sample.

due to the granularity of the material. By comparison with the results of Um et al. [7], who studied the c/a ratio and the transport properties of (Bi, Pb)$_2$Sr$_2$Ca$_2$Cu$_3$O$_{10+\delta}$ after anneals at 700°C in different oxygen pressures, we conclude that the as-prepared sample is close to being optimally doped.

After completing the XPS analysis following the last surface treatment (annealing in vacuum), the X-ray diffraction pattern was essentially equal to that of the as-grown sample [Fig. 1]. This indicates that the material is still single phase. The a-axis value is unaltered within our experimental accuracy of 0.002 Å, but the c-axis is slightly expanded to $c = 37.10 \pm 0.02$ Å.

The resistance curve as measured after the vacuum anneal has become non-linear above T_c, and the onset T_c is lowered to 105 K. The sample is fully superconducting below 89 K. Comparing these results with the oxygen-doping study of Um et al. [7] we see that the composition has moved into the direction of the metal-insulator transition. The narrowing of the Cu 2p$_{3/2}$ main peak as determined with XPS (discussed in the following section) also points into this direction [4]. It is important to notice, that the changes in the oxygen concentration at the sample surface are substantially larger than in the bulk, as follows from the intensities of the XPS lines. As the changes in μ are also measured with the same surface sensitive probe, we will use XPS as a quantitative

measure of both the oxygen stoichiometry as well as the doping dependence of the chemical potential.

3. Photoelectron spectra

After each treatment of the sample surface in a UHV chamber using the different procedures described above, the sample was immediately transported to the analysis chamber without breaking the ultra-high vacuum.

The core level and valence band spectra are displayed in Fig. 3. All spectra were measured with Mg Kα radiation and an analyser resolution of 0.4 eV. The carbon contamination was checked with 1 eV resolution, which gives a strongly increased sensitivity. The binding energies of the Bi 4f$_{7/2}$, Pb 4f$_{7/2}$, Sr 3d$_{5/2}$, Ca 2p$_{3/2}$, Cu 2p$_{3/2}$ and O 1s peaks of the as-prepared sample are 158.5, 137.4, 132.4, 345.0, 933.2 and 528.7 eV, respectively.

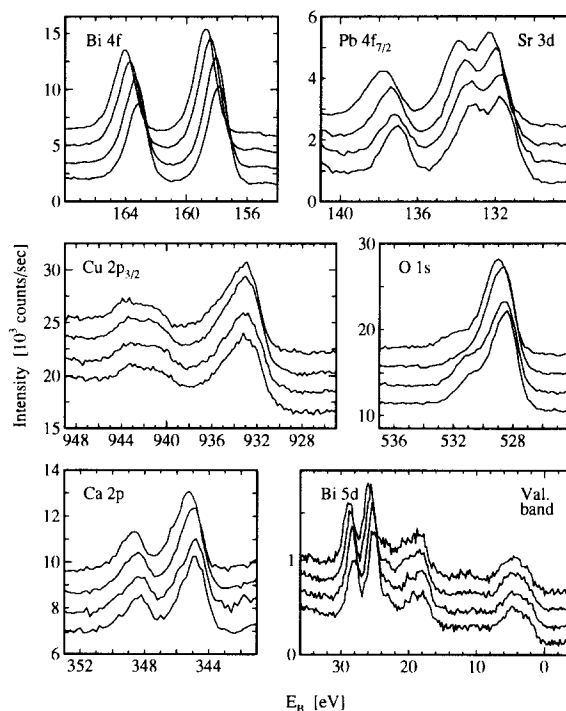Fig. 3. Core-level and valence-band spectra of the (Bi, Pb)$_2$Sr$_2$Ca$_2$Cu$_3$O$_{10+\delta}$ sample as a function of the O content. From top to bottom: spectra after treatment D, A, B, and C (see text). Spectra were given an offset for clarity. Note the systematic shift in *all* spectra, indicating a variation in chemical potential.

The Bi 4f spectrum consists of two multiplet-split peaks, which have a slight asymmetry towards higher binding energy, which can be taken as an indication of a coupling of the core levels to excited states in the metallic or semiconducting BiO blocking layers. Also the Pb $4f_{7/2}$ spectrum, shown in Fig. 3 together with the Sr 3d spectrum, has an asymmetric line shape. It is known that Pb substitutes for Bi in the $Bi_2Sr_2Ca_2Cu_3O_{10+\delta}$ superconductor. Unlike Golden et al. who find a larger asymmetry for Pb than for Bi [8], the 4f line shapes in our case are exactly the same. Although the spectra can be fitted to a Doniach–Šunjić-like line shape [9], due to limitations imposed by the life-time broadening of the XPS lines as well as instrumental broadening, the line shape may also be caused by a small semiconductor gap in the electron–hole shake-up tail. We observe that the line shape is insensitive to the oxygen content. Hence, if the asymmetry would be interpreted as a mixture of two valencies (Bi^{3+} and Bi^{5+}) of Bi in this compound [10,11], the average valency of Bi has to be independent on the degree of oxygenation. The shift of the Bi 4f level (also found in the Bi 5d spectra [Fig. 3]) is much larger than the shift of the Cu 2p spectrum. Also the core levels of Pb and Sr (which is next to the BiO planes) show a larger than average shift [Fig. 4]. This indicates that the extra oxygen is introduced
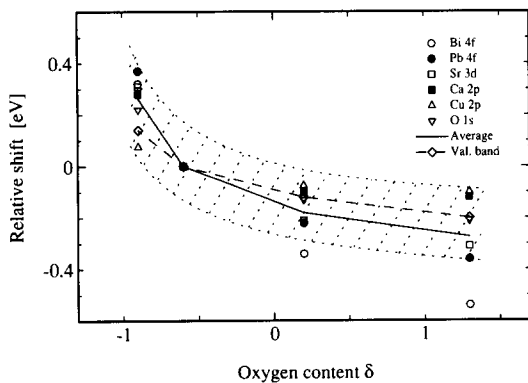

Fig. 4. Observed shifts in core-level and valence-band position of (Bi, Pb)$_2$Sr$_2$Ca$_2$Cu$_3$O$_{10+\delta}$ as a function of the oxygen content δ. Here, δ is the difference between the measured O content and that based on the total cation content of the material. From left to right on the horizontal axis are data after treatment D, A, B, and C. The solid line gives the average shift found in the core levels. The dashed line follows the change in valence band position. The dotted band indicates the scatter in the data (with the exception of Bi, see discussion in the text).

near the Bi and Pb atoms, supporting the point of view that the doping of the CuO$_2$ planes is controlled through the oxygen stoichiometry of the blocking layers. Together with the fact that the Bi line shapes remain unaffected, this indicates that the Bi core levels experience a decrease in binding energy due to the electrostatic potential surrounding the O^{2-} ions. In the Bi$_2$Sr$_2$Ca$_{1-x}$Y$_x$Cu$_2$O$_{8+\delta}$ material, the Y^{3+} ions replace the Ca between the CuO$_2$ planes, resulting in a shift of the Bi core level which is *smaller* than the average, as has also been observed experimentally [4,12].

The Sr 3d spectrum of Sr containing high-T_c superconductors is discussed extensively in Ref. [1]. The spectrum of the (Bi, Pb)$_2$Sr$_2$Ca$_2$Cu$_3$O$_{10+\delta}$ material resembles that of Bi$_2$Sr$_2$CaCu$_2$O$_{8+\delta}$ [1]. Thus either it consists of two components, one of them due to Sr–Ca disorder, or it has only one chemical component, with an asymmetric line shape.

A single doublet is seen in the Ca 2p spectrum, very similar to the early spectrum of Steiner et al. [13]. Later spectra of highly oriented and of single-crystalline Bi$_2$Sr$_2$CaCu$_2$O$_{8+\delta}$ material showed at least two spin–orbit-split pairs marking Sr–Ca disorder [10,14]. The unusual background in our spectrum is caused by Cu LMM Auger peaks.

In the Cu 2p$_{3/2}$ spectrum, there is the familiar double structure typical for Cu^{2+}. After treatment A (only scraping) the intensity ratio of satellite and main peak is 0.33, somewhat lower than for e.g. La$_{2-x}$Sr$_x$CuO$_4$. This ratio is almost independent of the oxygen treatment. After treatment D (annealing in vacuum) the main peak became somewhat narrower.

The O 1s core level is relatively broad, but in contrast with that of La$_{2-x}$Sr$_x$CuO$_4$ and YBa$_2$Cu$_3$O$_{7-\delta}$, almost free of a high binding-energy shoulder. Similar oxygen core-level spectra were measured on the Bi$_2$Sr$_2$CaCu$_2$O$_{8+\delta}$ material [11,15,16]. The large width of the peak is probably caused by slightly different binding energies of the different types of oxygen in the material, e.g. as predicted in band-structure calculations [17]. After treatment D a weak signal of carbon was present. All other treatments resulted in essentially carbon-free surfaces.

4. Doping dependence of the chemical potential

Clearly visible in Fig. 3 is the systematic shift of the spectra as a function of oxygen treatment. For a useful plot of this shift, a quantitative determination of the oxygen content is necessary. Using the calculated cross-section for each level [18] and assuming a random distribution of the elements in the sample, we find that the surface composition after scraping (treatment A) is $Bi_{2.2}Pb_{0.26}Sr_{2.0}Ca_{1.6}Cu_{2.8}O_{9.4}$, which is close to the nominal value in the bulk. In this chemical formula we scaled the cation content such as to make the total charge on the cations equal to $+20$, taking Bi^{3+}, Pb^{2+}, Sr^{2+}, Ca^{2+}, Cu^{2+} as the relevant formal valencies [19]. We define δ as the difference between the number of oxygen atoms based on the XPS peak intensities, and the number of O^{2-} ions required for total charge compensation of the cations. This we interpret as a quantitative measure of the *changes* in oxygen content. After treatments D, A, B, and C this is -0.9, -0.6, $+0.2$, and $+1.3$, respectively. The result of the shift in each core level versus δ is given in Fig. 4. As before [1], all shifts in the spectra are determined using the peak position, except for the Cu and the valence band spectrum where the leading edge of the spectrum is used. In the latter case, separate spectra (not shown in Fig. 3) with improved statistics were recorded using long counting times. Over the studied range of δ values, the average shift is reasonably linear with a small upturn after annealing in vacuum. By varying the source power during the XPS measurements we checked that the observed shifts in the spectra are not due to charging of the sample. In addition, there is no visible change in the shape of the spectra for different X-ray source powers, indicating that non-uniform charging of the surface debris left by scraping does not play a role as well.

Similar to $La_{2-x}Sr_xCuO_4$, the valence band follows the average core-level shift quite well, indicating that the observed shift is due to a variation of the chemical potential. We see from Fig. 4 that there is a clear shift in chemical potential when changing the oxygen content inside the metallic regime. The shift in μ as a function of doping is larger than in $La_{2-x}Sr_xCuO_4$ [1] and in the $Nd_{2-x}Ce_xCuO_4$ compounds [2]. This inconsistency would be removed if in the doped La and Nd copper oxides an additional band is formed within the charge-transfer gap, where the Fermi level remains pinned upon doping with holes or electrons. In principle such a band might exist due to the close proximity of the (disordered) layer of dopants to the metallic CuO_2 sheets. The doping layers are indeed further away in the $(Bi, Pb)_2Sr_2Ca_2Cu_3O_{10+\delta}$ system, which would then explain the absence (or a different binding energy) of such a band in these materials. The question whether such a band could indeed exist, poses an interesting theoretical challenge involving both a quantitative theory of the correlation induced insulating gap, and also a quantitative description of states within the gap induced by the dopant atoms. The fact that we observe a stronger shifting of μ upon approaching the metal–insulator transition is in general agreement with previous results with Y doping in $Bi_2Sr_2Ca_{1-x}Y_xCu_2O_{8+\delta}$ [4].

5. Conclusions

We studied the doping dependence of the chemical potential in $(Bi, Pb)_2Sr_2Ca_2Cu_3O_{10+\delta}$ as a function of O concentration δ with X-ray photoelectron spectroscopy. Differences between the Bi and Cu core-level shifts indicate that the oxygen enters the $(Bi, Pb)_2Sr_2Ca_2Cu_3O_{10+\delta}$ crystal structure closer to the Bi sites than to the Cu atoms. In the metallic regime the measured shift in μ is considerably larger than for the $La_{2-x}Sr_xCuO_4$ and $Nd_{2-x}Ce_xCuO_4$ system [2,3]. We observe that the chemical potential shifts more strongly, when we come closer to the metal–insulator transition by means of oxygen depletion. In general, our results on the $(Bi, Pb)_2Sr_2Ca_2Cu_3O_{10+\delta}$ system agree with those on Y doped $Bi_2Sr_2Ca_{1-x}Y_xCu_2O_{8+\delta}$ [4]. In terms of the present two model descriptions of the doping behavior of the chemical potential in the high-T_c superconductors, all data obtained on Bi containing high-T_c materials thus seem to support the "semiconductor model".

Acknowledgements

References

[1] G. Rietveld, M. Glastra and D. van der Marel, preprint (1994).

[2] J.W. Allen, C.G. Olson, M.B. Maple, J.-S. Kang, L.Z. Liu, J.-H. Park, R.O. Anderson, W.P. Ellis, J.T. Markert, Y. Dalichaouch and R. Liu, Phys. Rev. Lett. 64 (1990) 595.

[3] R.O. Anderson, R. Claessen, J.W. Allen, C.G. Olson, C. Janowitz, L.Z. Liu, J.-H. Park, M.B. Maple, Y. Dalichaouch, M.C. de Andrade, R.F. Jardim, E.A. Early, S.-J. Oh and W.P. Ellis, Phys. Rev. Lett. 70 (1993) 3163.

[4] M.A. van Veenendaal, R. Schlatmann, G.A. Sawatzky and W.A. Groen, Phys. Rev. B 47 (1993) 446.

[5] S.J. Collocott and R. Driver, Physica C 167 (1990) 598.

[6] H.M. Appelboom, PhD. thesis, Delft University of Technology, Department of Applied Physics (1992).

[7] W.S. Um, D.H. Kim, K. No and H.G. Kim, Jpn. J. Appl. Phys. 31 (1992) 775.

[8] M.S. Golden, D.A. Geeson, S.E. Male and W.R. Flavell, Supercond. Sci. Technol. 2 (1989) 185.

[9] S. Doniach and M. Šunjić, J. Phys. C 3 (1970) 285.

[10] F.U. Hillebrecht, J. Fraxedas, L. Ley, H.J. Trodahl, J. Zaanen, W. Braun, M. Mast, H. Petersen, M. Schaible, L.C. Bourne, P. Pinsukanjana and A. Zettl, Phys. Rev. B 39 (1989) 236.

[11] A. Fujimori, S. Takekawa, E. Takayama-Muromachi, Y. Uchida, A. Ono, T. Takahashi, Y. Okabe and H. Katayama-Yoshida, Phys. Rev. B 39 (1989) 2255.

[12] R. Itti, F. Munakata, K. Ikeda, H. Yamauchi, N. Koshizuka and S. Tanaka, Phys. Rev. B 43 (1991) 6249.

[13] P. Steiner, S. Hüfner, A. Jungmann, S. Junk, V. Kinsinger, I. Sander, W.R. Thiele, N. Backes and C. Politis, Physica C 156 (1988) 213.

[14] D.M. Hill, H.M. Meyer III, J.H. Weaver, C.F. Gallo and K.C. Goretta, Phys. Rev. B 38 (1988) 11331.

[15] Z.-X. Shen, P.A.P. Lindberg, B.O. Wells, D.B. Mitzi, I. Lindau, W.E. Spicer and A. Kapitulnik, Phys. Rev. B 38 (1988) 11820.

[16] H.M. Meyer III, D.M. Hill, J.H. Weaver, D.L. Nelson and C.F. Gallo, Phys. Rev. B 38 (1988) 7144.

[17] S. Massidda, J. Yu and A.J. Freeman, Physica C 152 (1988) 251.

[18] J.H. Scofield, J. Electr. Spectrosc. Relat. Phenom. 8 (1976) 129.

[19] M.S. Hegde and P. Ganguly, Phys. Rev. B 38 (1988) 4557.